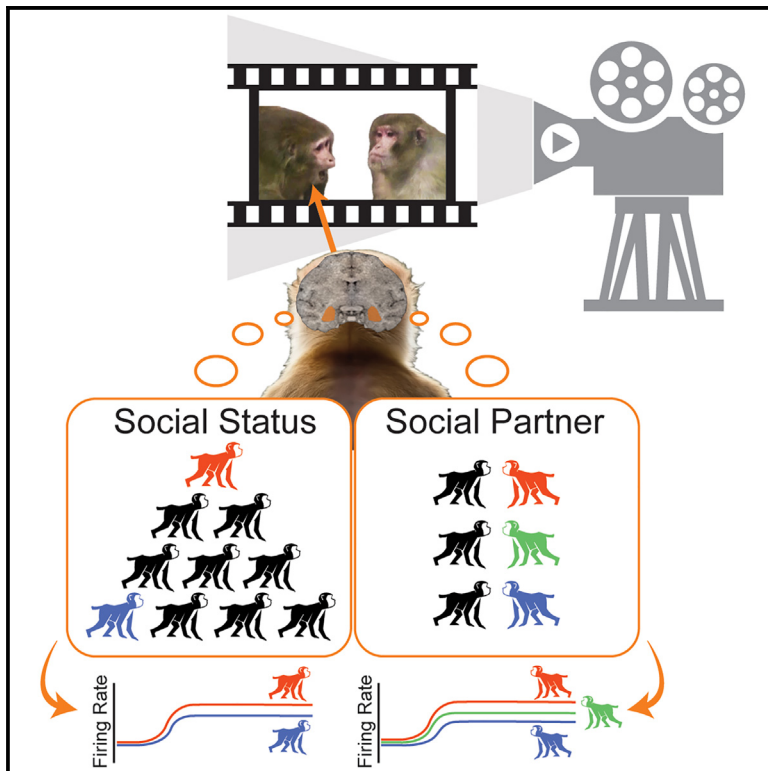


Neuron

Social status as a latent variable in the amygdala of observers of social interactions

Graphical abstract



Authors

SeungHyun Lee, Ueli Rutishauser,
Katalin M. Gothard

Correspondence

kgothard@arizona.edu

In brief

Third-party viewers of pairwise dominant-subordinate interactions infer social status from the observed behaviors. Neurons in the amygdala are tuned to the inferred dominant/subordinate status of both individuals.

Highlights

- Monkeys infer the social status of conspecifics from videos of dyadic interactions
- During fixations, neural populations signal the social status of attended individuals
- Neurons in the amygdala jointly encode the status of interacting individuals

Report

Social status as a latent variable in the amygdala of observers of social interactions

SeungHyun Lee,^{1,4} Ueli Rutishauser,^{2,3} and Katalin M. Gothard^{4,5,*}

¹Department of Neurosurgery, Massachusetts General Hospital, Harvard Medical School, Boston, MA 02114, USA

²Department of Neurosurgery, Cedars-Sinai Medical Center, Los Angeles, CA 90048, USA

³Computation and Neural Systems, Division of Biology and Biological Engineering, California Institute of Technology, Pasadena, CA 91125, USA

⁴Department of Physiology, College of Medicine, The University of Arizona, Tucson, AZ 85721, USA

⁵Lead contact

*Correspondence: kgothard@arizona.edu

<https://doi.org/10.1016/j.neuron.2024.09.010>

SUMMARY

Successful integration into a hierarchical social group requires knowledge of the status of each individual and of the rules that govern social interactions within the group. In species that lack morphological indicators of status, social status can be inferred by observing the signals exchanged between individuals. We simulated social interactions between macaques by juxtaposing videos of aggressive and appeasing displays, where two individuals appeared in each other's line of sight and their displays were timed to suggest the reciprocation of dominant and subordinate signals. Viewers of these videos successfully inferred the social status of the interacting characters. Dominant individuals attracted more social attention from viewers even when they were not engaged in social displays. Neurons in the viewers' amygdala signaled the status of both the attended (fixated) and the unattended individuals, suggesting that in third-party observers of social interactions, the amygdala jointly signals the status of interacting parties.

INTRODUCTION

High social status is one of the most coveted social commodities by both humans and non-human primates, as it ensures access to resources, reproductive success, social support, and, ultimately, better health and well-being.^{1–6} The desire to rise in a hierarchy or retain one's status, directly or indirectly shapes all interactions within a social group.^{7–12} These interactions rest on a mutual understanding of the social rules that govern relationships. By observing hierarchical interactions, primates learn to accurately place each member of their social group into a specific position on the social ladder, forming a linear hierarchy.^{13–17}

Macaque societies are distributed on a continuum between egalitarian societies (e.g., Tonkean macaques), where status plays a minor role in social interactions, and despotic societies, where strict linear hierarchies are enforced.^{18,19} Rhesus monkeys live in despotic societies,^{20,21} where status is established based on aggression and coalition-building skills in males, and the rank of the mother and birth order in females.^{22,23} Dominance is expressed through aggressive behaviors toward subordinates, whereas low status is expressed through appeasing displays.^{13,24,25} Thus, this species is ideally suited to explore the social-cognitive and neural foundations of social organization.

We investigated whether rhesus macaques can infer a social hierarchy from observing videos of simulated interactions among unfamiliar individuals. Given that in rhesus monkeys high status

is not exteriorized by morphological markers, such as skin or fur coloration,²⁶ the viewer monkeys were expected to infer status from observing pairwise interactions among “video monkeys” organized into an arbitrary linear hierarchy. To determine whether the behaviors in the videos elicited neural responses encoding social status, we recorded and analyzed the activity of neurons in the amygdala of two viewer monkeys. We hypothesized and confirmed that the inferred social status of the observed individual manifests in features of neural activity.

RESULTS

Looking time proportional to the status of the observed individuals

Two adult male monkeys, M_A and M_D, watched 740 and 928 videos, respectively, depicting dominant-subordinate dyadic interactions among unfamiliar monkeys organized into a hierarchy group. While they watched the videos, we recorded the viewers' scanpaths and single-unit activity from the amygdala (Figure 1A). Figures 1B and 1C illustrate that each hierarchy group consisted of four individuals, resulting in six pairwise interactions per group. We created four distinct hierarchy groups, totaling 24 videos. Each video was repeatedly watched, ranging from 58 to 74 repetitions. To simulate natural interactions, we juxtaposed pairs of videos, designating one monkey as dominant and the other as subordinate. The two monkeys appeared to be in

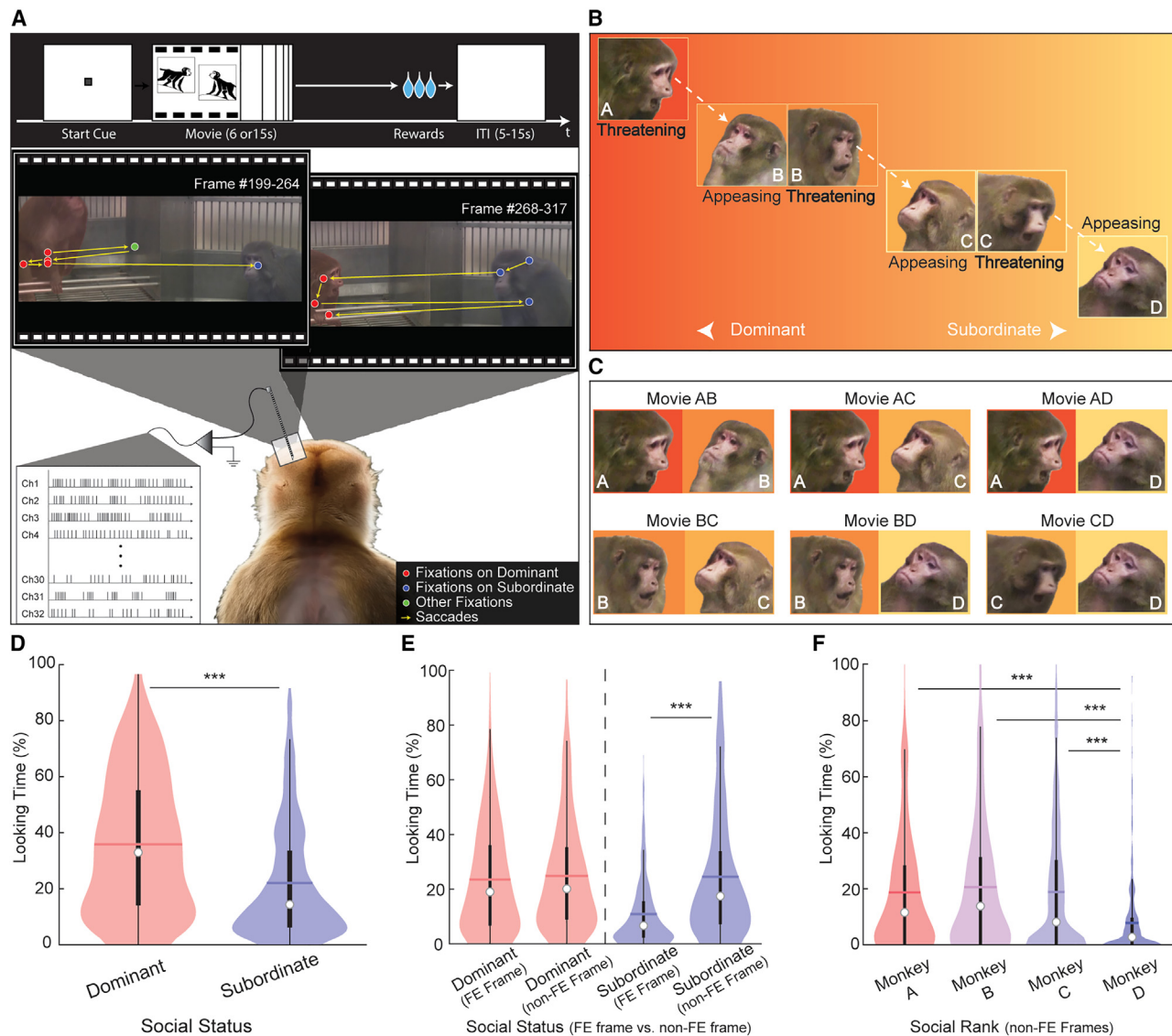


Figure 1. Experimental design, social interaction dynamics, and looking behavior analysis in viewer monkeys

(A) Viewer monkeys with electrode arrays in their amygdala watched videos depicting simulated pairwise social interactions. Each trial began with the viewer fixating on a start cue and receiving reward for watching the videos. Eye tracker recorded scanpaths (sequences of fixations and saccades). In two example scanpaths segments, red and blue circles denote fixations on dominant and subordinate monkeys, respectively, while yellow arrows represent the saccades connecting these fixations.

(B) An example linear hierarchy constructed from juxtaposed videos of aggressive and appeasing displays of four male monkeys (A, B, C, and D).

(C) Pairwise interactions among monkeys A, B, C, and D. Monkey A consistently displayed threatening behavior toward all partners, while monkey D consistently exhibited appeasing behavior toward all partners. Monkeys B and C alternated between dominant and subordinate roles, depending on their social partner.

(D) Proportion of cumulative fixation duration on dominant and subordinate individuals relative to the total playing time of the movie (15 s) (***: $p < 0.001$).

(E) Proportion of looking time at frames depicting facial expressions (FE) and neutral faces (non-FE) relative to the total screen time of FE and non-FE frames (***: $p < 0.001$).

(F) Proportion of cumulative looking time at neutral faces of each hierarchical individual relative to the total screen time of frames with neutral faces (***: $p < 0.001$).

each other's line of sight, and the timing of the threatening-appeasing displays was adjusted to simulate the natural cycle of dominant-subordinate signal exchanges.

We analyzed the average time viewers spent looking at each monkey in the dyad and compared the proportion of time spent looking at the dominant and subordinate animals in each video

(see STAR Methods for calculation details in Figures 1D–1F). On average, the viewer monkeys spent more time looking at the dominant animal (mean: $\mu = 35.87\%$, standard deviation: $\sigma = 24.18\%$) than the subordinate animal ($\mu = 22.07\%$, $\sigma = 20.19\%$) in the dyad (Figure 1D; t test, $t(4,534) = 20.86$, $p = 2.41 \times 10^{-92}$). The threatening facial expressions produced by

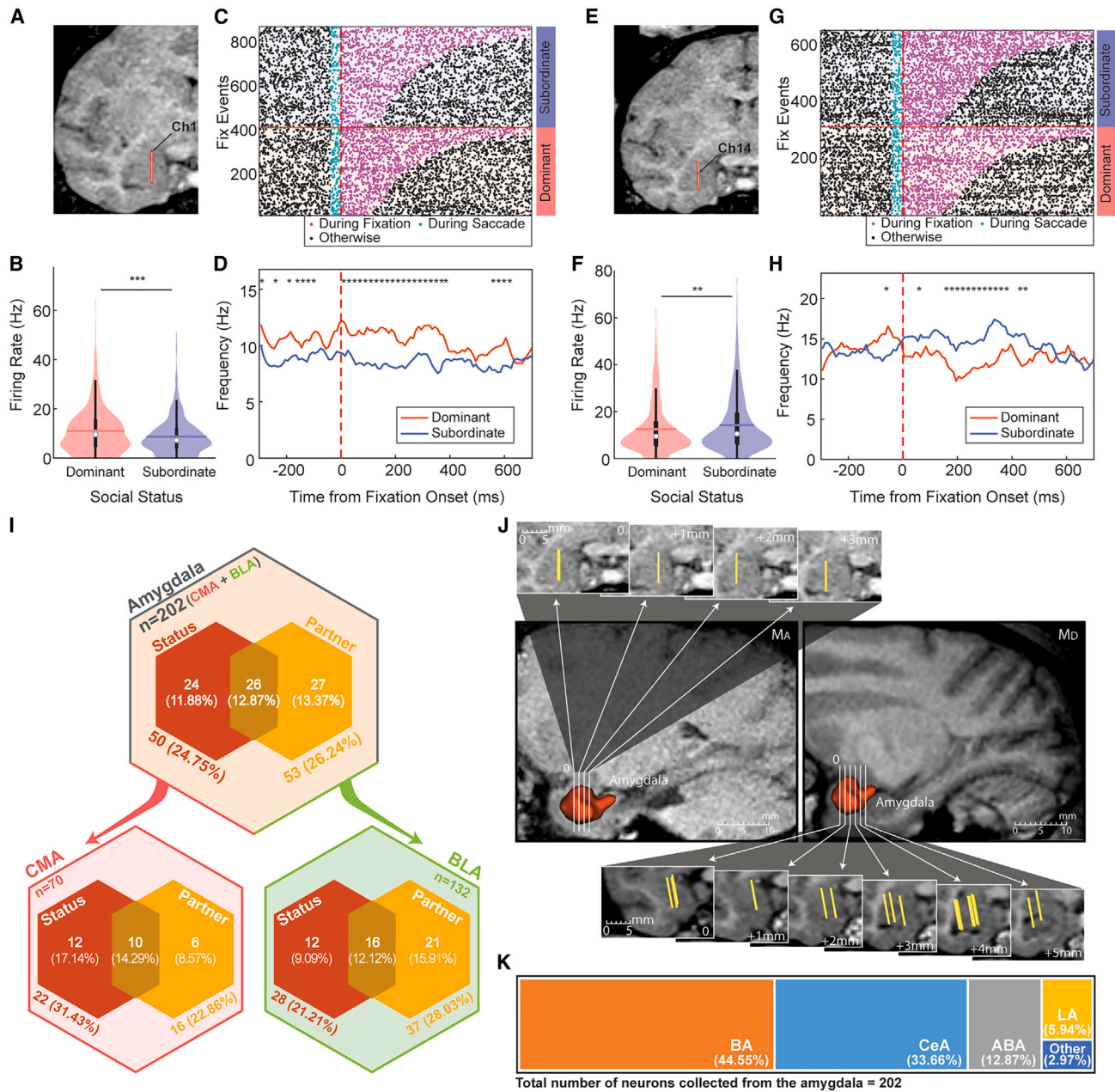


Figure 2. Neuronal tuning to social status in the amygdala

(A–H) Coronal MRI slices in (A) and (E) indicate the position of a 32-contact V-probe in the amygdala, marked by red lines. (A)–(D) depict the neuron recorded from channel 1 in the central nucleus, whereas (E)–(H) show an example neuron recorded from channel 14 located in the basal nucleus.

(B) Firing rates were significantly higher during fixations on dominant animals (***: $p < 0.001$).

(C) Raster plot showing fixations on subordinate (top) and dominant (bottom) animals in a dyad, sorted by fixation duration. Magenta dots represent spikes during fixations, and cyan dots represent spikes during preceding saccades (with saccade durations ranging from 36 to 54 ms).

(D) Temporal pattern of status-related responses in a fixation-aligned histogram of firing rates, indicating time bins with significantly higher firing rates during fixations on dominant animals (0–400 ms).

(F) Firing rates during fixations on the subordinate animals were significantly higher (**: $p < 0.01$).

(G) Separate rasters for fixations on subordinate (top) and dominant (bottom) animals in a dyad, sorted by fixation duration.

(H) Temporal pattern of status-related responses in a fixation-aligned histogram of firing rates, indicating time bins with significantly lower firing rates during fixations on dominant animals (0–400 ms).

(legend continued on next page)

the dominant animals do not account for the longer looking times, as comparable looking times were elicited by threatening ($\mu = 21.29\%$, $\delta = 19.73\%$) or neutral facial expressions ($\mu = 21.00\%$, $\delta = 21.56\%$) of the dominant animal (red violin plots in Figure 1E; t test, $t(1,501) = 0.27$, $p = 0.79$). Moreover, viewers allocated less attention to subordinate animals when they displayed appeasing facial expressions ($\mu = 9.01\%$, $\delta = 11.53\%$) compared with neutral facial expressions ($\mu = 14.43\%$, $\delta = 23.46\%$) (blue violin plots in Figure 1E; t test, $t(1,353) = -5.56$, $p = 3.30 \times 10^{-8}$), suggesting that viewers allocate attention to, and gain information from, both neutral and dominant/subordinate displays (see also Figure S1). Indeed, when comparing viewers' looking times at the neutral faces of the four monkeys in the hierarchy, the least-fixed neutral faces were those of the lowest-ranking monkey, D (Figure 1F), while the differences among the other monkeys were not significant (one-way ANOVA with factor identity, $df = 3$, $F = 21.38$, $***: p < 0.001$, A vs. B: $p = 0.63$, A vs. C: $p = 1.00$, A vs. D: $p = 1.64 \times 10^{-9}$, B vs. C: $p = 0.70$, B vs. D: $p = 7.11 \times 10^{-13}$, C vs. D: $p = 1.74 \times 10^{-9}$). These findings collectively suggest that increased social attention primarily reflects the individual's social status rather than merely their identity or facial expressions alone.

Neurons in the amygdala respond to social status of the attended individuals

We recorded neural activity of 202 well-isolated single neurons in the amygdala of two viewer monkeys. Our goal was to determine whether the neural activity elicited by watching the videos carries information about the social status of the protagonists. Specifically, we compared the firing rates during fixations on the faces or bodies of dominant and subordinate monkeys. Prior to analyzing the contribution of social status to neural activity in the amygdala, we verified that these videos elicited neuronal responses that are comparable with previously documented responses to static images or videos of single individuals^{27,28} and to multiple faces presented simultaneously.²⁹ As expected, a two-way ANOVA analysis (factors: identity and facial expression, see STAR Methods) replicated previous findings: 28.22% of amygdala neurons were selective for individual faces/bodies, fewer (7.92%) were selective for facial expressions, and a subclass of neurons (5.94%) showed mixed selectivity for both identity and facial expression.

Figure 2 shows two example status-responsive neurons recorded from the central (Figures 2A–2D) and accessory basal (Figures 2E–H) nuclei of the amygdala. We analyzed firing rates during fixations on dominant versus subordinate individuals, independent of the fixation target's identity and order of fixation. As the status of the mid-ranking monkeys B and C depended on the social partner, we analyzed fixations separately according to each individual's social status in each video pair. In the first example neuron, firing rates during fixations on dominant animals ($\mu = 11.00$ Hz, $\delta = 9.19$ Hz) were significantly higher across all dominant animals in the six pairwise interactions (Figure 2B;

t test, $t(856) = 4.13$, $p = 3.97 \times 10^{-5}$) compared with fixations on subordinate animals ($\mu = 8.66$ Hz, $\delta = 7.39$ Hz). Conversely, in the second example neuron, firing rates during fixations on the subordinate animals ($\mu = 15.37$ Hz, $\delta = 12.20$ Hz) were higher (Figure 2F; t test, $t(655) = -3.16$, $p = 1.70 \times 10^{-3}$) than during fixations on dominant animals ($\mu = 12.49$ Hz, $\delta = 11.05$ Hz). This was the case despite the great heterogeneity of fixation targets (various individuals, facial expressions, and face or body areas). The temporal patterns of status-related responses were analyzed using fixation-aligned histograms of firing rates, indicating time bins where the firing rates were significantly higher when viewing dominant animals (Figure 2D; t test with sliding window, bin size = 60 ms, stride size = 10 ms, $*: p < 0.05$). Another histogram (Figure 2H; employing the same methods as in Figure 2D) highlighted time bins with lower firing rates when fixating on dominant animals. Notably, fixations in Figures 2C and 2G can be preceded by fixations on either dominant or subordinate individuals, thus it was possible to detect significantly different firing rates in the time bins preceding the fixation onset (time 0). Nevertheless, both neurons exhibited tuning to the social status of the currently fixated individual. At the population level, 24.75% of recorded amygdala neurons (50 out of 202) responded with significant changes in firing rates to either dominant or subordinate status, and these neurons were distributed across both the centromedial and basolateral nuclei of the amygdala (Figure 2I). Neurons included in these analyses were recorded from all the major amygdala nuclei, predominantly localized in the basal and central nuclei (Figures 2J and 2K).

Status emerges as a latent variable in neural activity, alongside manifest variables like face identity, indicating mixed selectivity. For monkeys A and D, ranked highest and lowest in the hierarchy, respectively, identity and social status were not dissociable because of their consistent dominance or subordination across all three partners. However, face identity and social status could be dissociated in mid-ranking monkeys B and C, as they alternated between dominant and subordinate roles, depending on the partner (Figures 1B and 1C). A two-way ANOVA analysis (factors: social status and identity) of fixation-related firing rates while viewing monkeys B and C showed not only a main effect of status (16.83% of recorded neurons) but also a main effect of identity (20.79% of recorded neurons), along with a significant status-identity interaction (13.86% of recorded neurons). Given that close to 25% of recorded neurons showed tuning to social status, the small effects at the level of individual neurons may amount to large signals at the population level (Figure 2I). To test this hypothesis, we conducted a group analysis of all neurons.

Status-related population responses in the amygdala

We used demixed principal component analysis (dPCA)^{30,31} to determine status-related changes in population firing rates of all recorded neurons during fixations on each monkey. This supervised approach captures the variance in population activity explained by two factors and their interaction: *movie* (the six

(I) Venn diagram showing the proportion of amygdala neurons (CMA, BLA, and total) tuned to social status (significant firing rate changes when fixating on dominant or subordinate targets) and social context (partner effect: significant firing rate changes in response to the fixation target's partners).

(J) Recording locations in M_A and M_B, with yellow bars indicating electrode positions across all 23 recorded sites from 20 recordings.

(K) Distribution ratio of collected amygdala neurons among different subregions ($n = 202$).

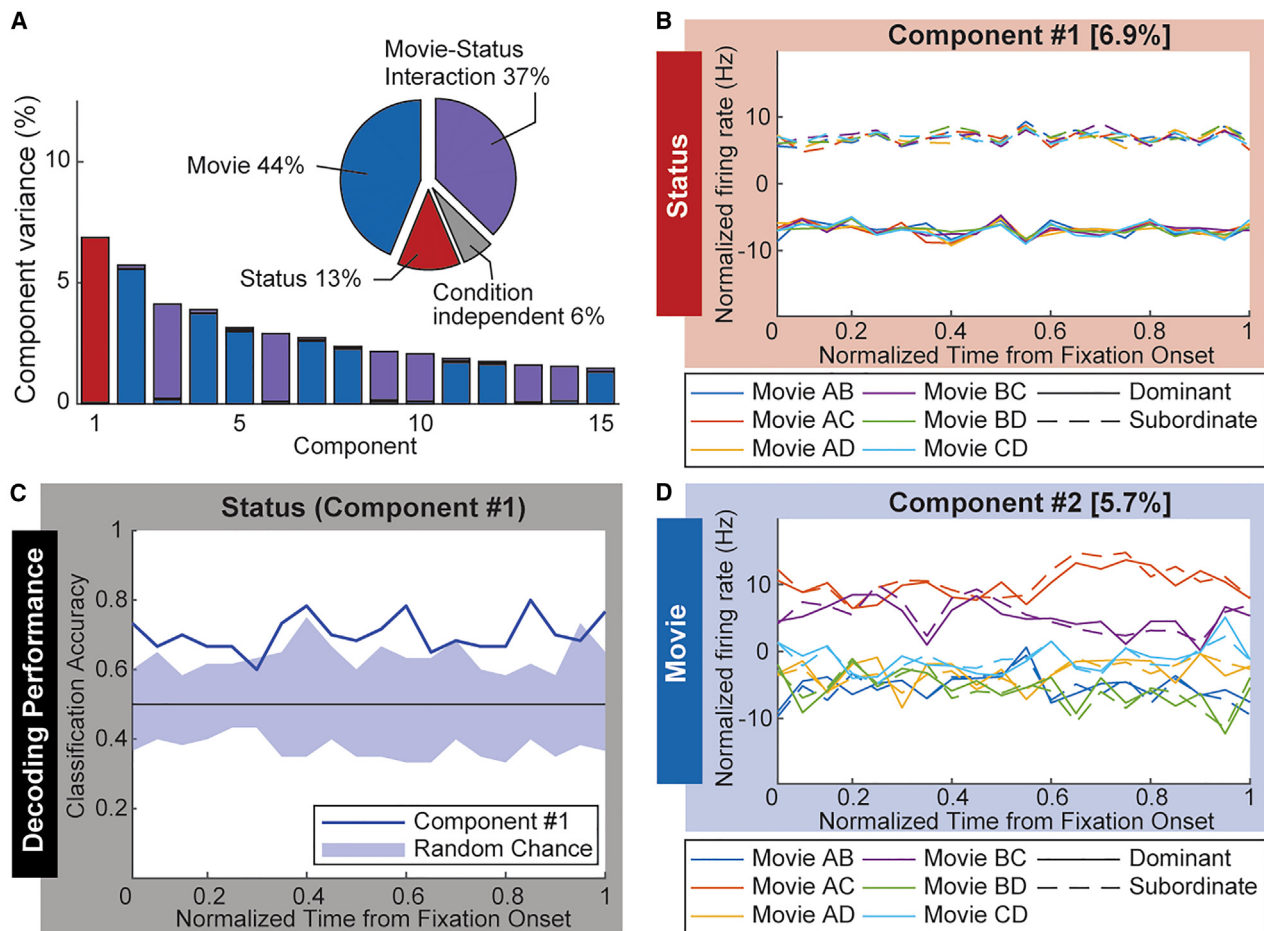


Figure 3. dPCA reveals the primacy of social status in neural population activity during fixations

(A) Proportion of variance explained by each component (left) and factor (inset). Each “Movie” refers to one of the six distinct video clips featuring different dyads. (B) Normalized firing rate of the first dPCA component (#1) as a function of time, movie identity (color), and social status of the fixated animal (straight/dashed line). This single component explained 6.9% of overall variance. Note how the normalized firing rates for all subordinates (dashed lines) are distinct from those of all dominants (solid lines) across all movie types, indicating encoding of social status.

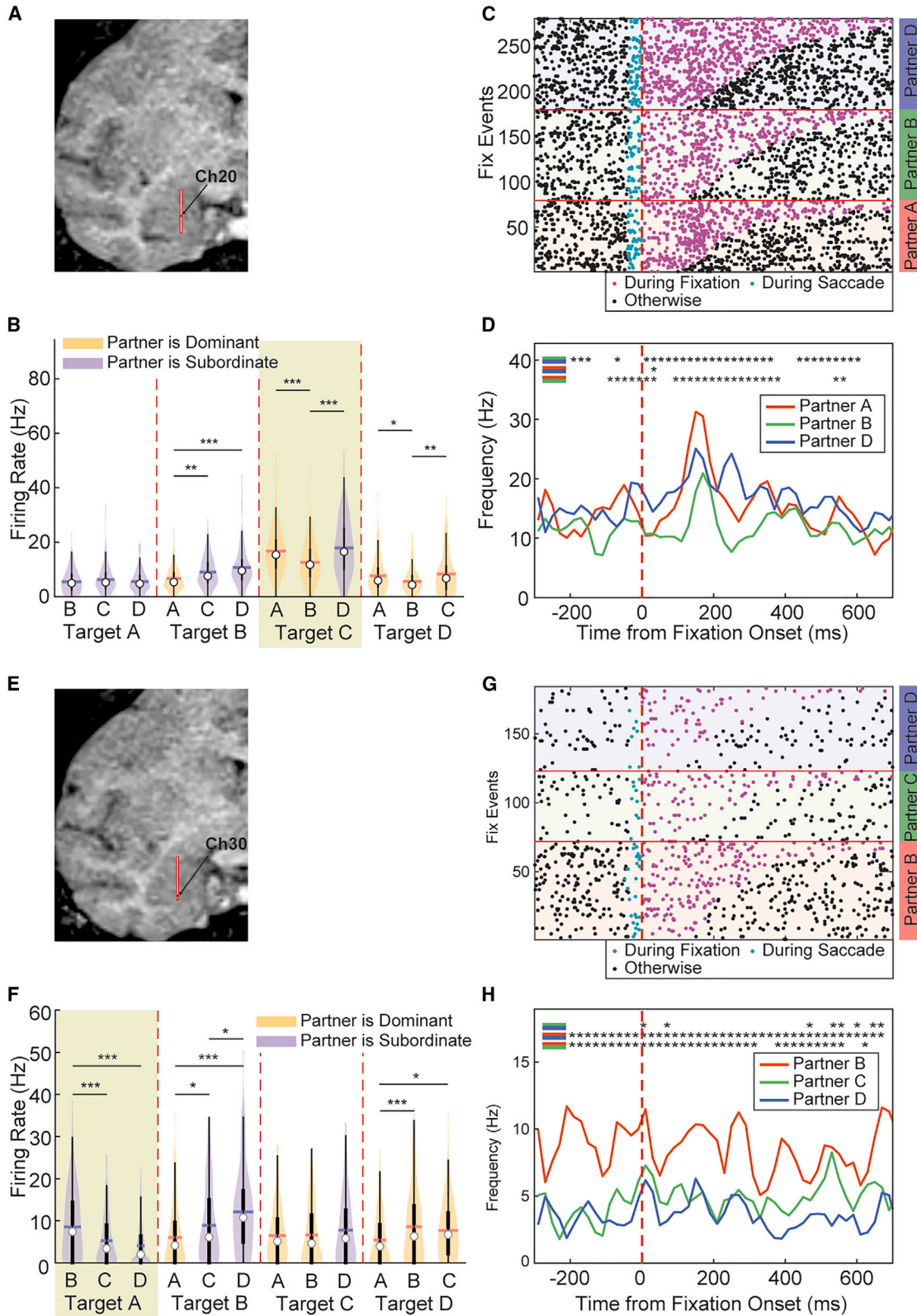
(C) Classification of social status based on activity projected along component 1. Decoding was significantly above chance, indicating that amygdala firing rates during fixations are influenced by the social status of the target. The shaded area represents the range of classification accuracy expected by chance, estimated from 100 shuffling iterations, while the solid line indicates the classification accuracy of component #1. Only this component’s decoding performance was significantly larger than expected by chance.

(D) Normalized firing rate of the second dPCA, which represents “Movie” type (#2), as a function of time. This component explained 5.7% of variance. Note how activity differed as a function of movie type (color) but not social status (straight vs. dashed lines). The color code shown below (D) indicates that different colors indicate movie types, with solid lines for dominants and dashed lines for subordinates. It applies to both (D) and (B). $t = 0$ is fixation onset throughout.

dyads) and *status* (dominant and subordinate). Across all dPCA components, *status* (13%) and *movie* (44%) explained the largest variance in neural activity, followed by their interaction (37%) (Figure 3A). This finding aligns with the observation that status-related responses varied with the social partner (partner effect), as each movie depicted a different pairing of four animals in the hierarchy. To incorporate fixations with varying durations into the dPCA model, we normalized the duration of each fixation to a unit time of 1 s, segmented into 20 time points. The first dPCA component (*status*, red box, Figure 3B), explains 6.9% of the variance in the neural response. Examining the response projected onto this dPCA component reveals clear separation of the response between fixations on dominant (solid lines) and

subordinate (dotted lines) monkeys for all six movies (Figure 3B). This result was further supported by the ability to decode social status reliably from the neural activity projected onto the first dPCA component (Figure 3C).

Further, the second dPCA component (*movie*, blue box, Figure 3D) explains 5.7% of the variance in the neural response. Examining activity as a function of time along this component reveals separation between movies AC and BC (orange and purple lines) from the other four movies but not between social status (Figure 3D). In these movies, one side shows monkey C appeasing monkeys A and B. Component #2 likely segregates the appeasing behavior, rather than just the identity, of monkey C, as movie CD, which depicts monkey C threatening, does not separate out in this



(legend on next page)

component. In contrast to social status (component #1), movie identity was not decodable (Figure S2). Therefore, despite explaining similar amounts of variance, social status was more robust at the population level to that of movie identity.

The dPCA results showed that, beyond face identity and facial expression, the population of neurons in the amygdala, whether individually tuned to status or not, contains information about the status of interacting individuals and the specific video being watched. As a control, we repeated the dPCA analysis on amygdala recordings, while subjects watched videos of moving objects formatted identically to the hierarchy movies. In this control condition, classification accuracy for “status” did not surpass chance levels when status was arbitrarily assigned to moving objects (Figure S3).

The partner effect: Neural responses to the status of the attended individual are modulated by the status of the unattended individual

We asked whether the status-related response during fixation on a dominant or subordinate monkey was different when the partner was different. If the firing rates while looking at the same animal displaying the same behaviors are fully explained by the content of the viewed video, the identity of the social partner should not alter the observed neural responses. Recall that the same videos were used to depict the dominant or subordinate behaviors of each monkey in the hierarchy (the same video depicted monkey A as dominant to monkeys B, C, and D). Thus, fixations on monkey A (the highest-ranking animal) are expected to elicit the same firing rates regardless of whether the partners are monkeys B, C, or D. Contrary to this prediction, however, we found a “partner effect” in 26.2% of the 202 amygdala neurons (i.e., a significant main effect of social partner on the firing rate of the fixated individual, computed using one-way ANOVA). Figure 4 shows two example neurons that illustrate this partner effect.

The neuron shown in Figures 4A–4D exhibits a strong partner effect when looking at monkey C, where the firing rate increases when the partner is D compared with B, and also increases when the partner is A compared with B (one-way ANOVA, $df = 2$, $F = 9.07$, $***: p < 0.001$). Furthermore, this neuron shows a strong fixation-related increase in neural activity at a latency of approximately 100 ms after fixation onset on monkey C, but this activity is suppressed when the partner is monkey B (Figure 4D). In the second example neuron (Figures 4E–4H), firing rates during fixation on monkey A are higher when the partner is B than C or D,

despite all three partners displaying similar appeasing expressions. Note that the firing rate in response to fixating on monkey A decreases as the status of the social partner decreases (one-way ANOVA, $df = 2$, $F = 10.42$, $***: p < 0.001$). Likewise, firing rates during fixations on monkey D are lower when the partner is A compared with B and C.

The partner effect was present in 53 out of 202 monitored neurons (26.2%), a proportion comparable with the 24.7% neurons that showed a status effect (Figure 2I). Comparable proportions of neurons showed only a status effect, only a partner effect, and mixed selectivity for both (11.8%, 12.8%, and 13.3%, respectively). Overall, the partner effect suggests a joint representation of the two monkeys, where one animal serves as the focal point of the viewer’s social attention while the other provides the “social context” in which the viewed individual is processed. This reflects the complex interplay between social status and social interactions encoded in amygdala neuronal activity.

DISCUSSION

Here, we report that macaque viewers of dyadic interactions extracted the social status of the observed individuals and expressed their knowledge by allocating increased social attention toward dominant individuals. Indeed, in social tasks, humans and macaques look more at high-status individuals.^{11,12,32–38} This looking preference did not emerge simply from more fixations on facial expressions, as the threatening and neutral faces of dominant individuals received similar levels of attention, neither was it informed by visible features of status, such as face coloration in mandrills.³⁹ In rhesus macaques, these visible features are either unrelated²⁶ or weakly related to social status.^{40,41} Remarkably, despite the artificial nature of the stimuli, the viewers extracted the status of each monkey, suggesting that for rhesus monkeys, understanding social status is paramount and even incomplete information is sufficient to acquire this knowledge. Compared with the robust effect of status, the full hierarchical ranking ($A > B > C > D$) did not emerge from the scanpaths or neural responses. Such complex representations may require transitive inference training or the simultaneous observation of all four members of the hierarchy.

Social status as a latent variable in neural activity

In response to the static images of faces, neurons in the amygdala of both humans and monkeys respond to face identity,^{27,29,42–44}

Figure 4. Neurons showing the partner effect

The red line superimposed on the coronal MRI slices in (A) and (E) indicates the position of a 32-channel V-probe in the amygdala and the closest contact to the example neuron. (A)–(D) depict the neuron recorded from channel 20 in the accessory basal nucleus, whereas (E)–(H) show an example neuron recorded from channel 30 located in the basal nucleus.

(B) Each triplet of violin plots depicts firing rates during fixation on a monkey from the hierarchy (target A, B, C, and D) with each possible partner. The first triplet represents firing rates during fixations on monkey A with partners B, C, and D. The second triplet (separated by red dotted lines) represents firing rates during fixations on monkey B with partners A, C, and D. Partner status relative to the fixated individual is color-coded yellow for dominant and blue for subordinate. Bars and stars correspond to the statistically significant differences (one-way ANOVA, *: $p < 0.05$, **: $p < 0.01$, ***: $p < 0.001$).

(C) Rasters of spike trains aligned to the onset of fixations on the middle-ranking monkey C (triplet with lime green background in B), paired with monkeys A (red), B (green), and D (blue).

(D) Fixation-aligned firing-rate histogram corresponding to the raster in (C); using t test between pairs of sliding windows, as indicated by color legend in the upper left corner (bin size = 60 ms, stride size = 10 ms, *: $p < 0.05$).

(E–H) The same plots for a neuron located in the basal nucleus. The violin plots with the lime green background correspond to the triplet of fixating monkey A while paired with B, C, and D, as indicated by the red, green, and blue boxes and lines in (G) and (H) (*: $p < 0.05$, **: $p < 0.01$, ***: $p < 0.001$).

facial expressions,²⁷ and even the social status of familiar individuals within a hierarchy known to the viewer.⁴⁵ When the observers and the observed have a history of interactions, conditioning can explain the status-related responses. By comparison, the novelty of our study is the emergence of inferred social status through observing interactions among unfamiliar individuals. In our paradigm, status inference may have been facilitated by videos of simulated interactions, which contain more useful information than static portraits of known individuals (see [Figure 1](#)). The amygdala also contributes to learning the relative status of individuals in a hierarchy.⁴⁶ Because one of our subjects (M_D) was familiar with these videos by the time neural recordings started, we were unable to track the emergence of the status-related neural responses. In a prior study,¹² M_D was more likely to produce joint-attention saccades from the eyes and faces of the subordinate monkeys, indicating a prior understanding of the status of each animal.

At the level of individual neurons, status is a distinct variable, differentiating between fixations on dominant and subordinate animals. This variable may, in essence, be equivalent to identity and facial expressions, contributing to the mixed selectivity of amygdala neurons.^{47–52} Higher social status was not always associated with higher firing rates, as shown in [Figures 2E–2H](#). Response suppression as a form of stimulus selectivity has been well documented in the amygdala⁵³ and is related to features of circuit architecture that support highly complex behaviors through disinhibition.⁵⁴ At the neural population level, status emerged as a distinct, abstract variable only when watching videos of interacting monkeys, not objects ([Figures S2 and S3](#)). However, status was a latent rather than a manifest variable, inferred through dPCA from firing rates during fixations on the observed pair, unlike explicit stimulus parameters such as threatening faces.

Neurons in the amygdala jointly represent the status of interacting individuals

Our findings add an additional, novel dimension to the role of the amygdala in social perception. Not only do individual neurons respond to the social status of the attended individual but their responses also depend on the unattended individual, who serves as a context signal. Context in this case is the presence of a specific individual, as shown previously for social and affective touch.⁵⁵ Indeed, the amygdala emerged as a key node for processing social status since the earliest lesion studies in non-human primates. Without an intact amygdala, monkeys fall in the social hierarchy^{56–58} and fail to display status-appropriate behaviors.^{59–61}

It is possible, although not tested in this study, that the observed behaviors and neural responses are also informed by the viewer's subjective status relative to the status of the observed individual, reflecting a self-centered versus other-centered status representation.⁶² Self-status is reflected in gray matter density in the amygdala⁶³ and in fMRI signals.^{64,65} Similar effects have been shown in humans: lower perceived socioeconomic status causes greater activation of the amygdala.⁶⁶ Self-status may be driven by subjective experiences, such as gains and losses during confrontations, which shape an individual's expectations for future interactions and prepare the individ-

ual to extend these expectations to social partners. In species with strictly linear hierarchies, the status of others is among the defining features of an individual, akin to age, sex, and physical appearance, that informs virtually all social behaviors.

RESOURCE AVAILABILITY

Lead contact

Further information and requests for resources and reagents should be directed to and will be fulfilled by the lead contact, Katalin M. Gothard (kgothard@arizona.edu).

Materials availability

This study did not generate new unique reagents.

Data and code availability

The data and original codes have been deposited at Figshare and are publicly available as of the date of publication. DOIs are listed in the [key resources table](#). Any additional information required to reanalyze the data reported in this paper is available from the [lead contact](#) upon request.

ACKNOWLEDGMENTS

This study was funded by NIH grant P50MH100023. We thank Tess M. Champ, Derek O'Neill, Natalia Magnusson, and Dr. Blake T. Seaton for help with animal training and data collection. Michael A. Cardenas and Archer I. Bowman provided manuscript editing. We also extend our gratitude to the University Animal Care (UAC) veterinary staff at the University of Arizona.

AUTHOR CONTRIBUTIONS

Experimental design: S.L. and K.M.G.; data collection: S.L.; data analysis and interpretation: S.L., K.M.G., and U.R.; manuscript preparation: S.L., K.M.G., and U.R.

DECLARATION OF INTERESTS

The authors declare no competing interests.

STAR★METHODS

Detailed methods are provided in the online version of this paper and include the following:

- [KEY RESOURCES TABLE](#)
- [EXPERIMENTAL MODEL AND STUDY PARTICIPANT DETAILS](#)
 - Subject Details
 - Video Stimuli
 - Task flow
- [METHOD DETAILS](#)
 - Collecting Eye Tracking Data and Processing
 - Equations for the Looking Time Analysis
- [QUANTIFICATION AND STATISTICAL ANALYSIS](#)
 - Single-unit Spike Recording and Identification of Stable Cells
 - Quantifying Cell Responses Tuned to Social Status and Partner Effect
 - Statistics
- [ADDITIONAL RESOURCES](#)
 - Visualizing Data Set Distributions

SUPPLEMENTAL INFORMATION

Supplemental information can be found online at <https://doi.org/10.1016/j.neuron.2024.09.010>.

Received: July 3, 2024
Revised: August 12, 2024
Accepted: September 10, 2024
Published: October 9, 2024

REFERENCES

- Rodriguez-Llanes, J.M., Verbeke, G., and Finlayson, C. (2009). Reproductive benefits of high social status in male macaques (Macaca). *Anim. Behav.* 78, 643–649. <https://doi.org/10.1016/j.anbehav.2009.06.012>.
- Vandeleest, J.J., Beisner, B.A., Hannibal, D.L., Nathman, A.C., Capitanio, J.P., Hsieh, F., Atwill, E.R., and McCowan, B. (2016). Decoupling social status and status certainty effects on health in macaques: a network approach. *PeerJ* 4, e2394. <https://doi.org/10.7717/peerj.2394>.
- Muscattell, K.A., Dedovic, K., Slavich, G.M., Jarcho, M.R., Breen, E.C., Bower, J.E., Irwin, M.R., and Eisenberger, N.I. (2016). Neural mechanisms linking social status and inflammatory responses to social stress. *Soc. Cogn. Affect. Neurosci.* 11, 915–922. <https://doi.org/10.1093/scan/nsw025>.
- Shively, C.A., and Wilson, M.E. (2016). *Social Inequalities in Health in Nonhuman Primates* (Springer Cham).
- Chiao, J.Y. (2010). Neural basis of social status hierarchy across species. *Curr. Opin. Neurobiol.* 20, 803–809. <https://doi.org/10.1016/j.conb.2010.08.006>.
- Snyder-Mackler, N., Sanz, J., Kohn, J.N., Brinkworth, J.F., Morrow, S., Shaver, A.O., Grenier, J.C., Pique-Regi, R., Johnson, Z.P., Wilson, M.E., et al. (2016). Social status alters immune regulation and response to infection in macaques. *Science* 354, 1041–1045. <https://doi.org/10.1126/science.aah3580>.
- Hawley, P.H. (1999). The ontogenesis of social dominance: A strategy-based evolutionary perspective. *Dev. Rev.* 19, 97–132. <https://doi.org/10.1006/drev.1998.0470>.
- Cheney, D.L., and Seyfarth, R.M. (1990). *How Monkeys See the World: Inside the Mind of Another Species* (University of Chicago Press).
- Hawkey, L.C., and Capitanio, J.P. (2015). Perceived social isolation, evolutionary fitness and health outcomes: a lifespan approach. *Philos. Trans. R. Soc. Lond. B Biol. Sci.* 370, 20140114. <https://doi.org/10.1098/rstb.2014.0114>.
- Maestriperi, D., and Hoffman, C.L. (2012). *Behavior and Social Dynamics of Rhesus Macaques on Cayo Santiago*. In *Bones, Genetics, and Behavior of Rhesus Macaques*. *Developments in Primatology: Progress and Prospects*, Q. Wang, ed. (Springer), pp. 247–262.
- Shepherd, S.V., Deaner, R.O., and Platt, M.L. (2006). Social status gates social attention in monkeys. *Curr. Biol.* 16, R119–R120. <https://doi.org/10.1016/j.cub.2006.02.013>.
- Champ, T.M., Lee, S., Martin, A.B., Bolles, C.M., Kim, S.W., and Gothard, K.M. (2022). Social engagement revealed by gaze following in third-party observers of simulated social conflict. *Front. Psychol.* 13, 952390. <https://doi.org/10.3389/fpsyg.2022.952390>.
- de Waal, F.B. (1986). The integration of dominance and social bonding in primates. *Q. Rev. Biol.* 61, 459–479. <https://doi.org/10.1086/415144>.
- Whiten, A., and Byrne, R.W. (1988). *The Manipulation of Attention in Primate Tactical Deception*. In *Machiavellian Intelligence: Social Expertise and the Evolution of Intellect in Monkeys, Apes, and Humans*, R.W. Byrne and A. Whiten, eds. (Clarendon Press/Oxford University Press), pp. 211–223.
- Perry, S., Baker, M., Fedigan, L., Gros-Louis, J., Jack, K., MacKinnon, K.C., Manson, J.H., Panger, M., Pyle, K., and Rose, L. (2003). Social Conventions in Wild White-faced Capuchin Monkeys: Evidence for Traditions in a Neotropical Primate. *Curr. Anthropol.* 44, 241–268. <https://doi.org/10.1086/345825>.
- Canteloup, C., Hoppitt, W., and van de Waal, E. (2020). Wild primates copy higher-ranked individuals in a social transmission experiment. *Nat. Commun.* 11, 459. <https://doi.org/10.1038/s41467-019-14209-8>.
- Canteloup, C., Cera, M.B., Barrett, B.J., and van de Waal, E. (2021). Processing of novel food reveals payoff and rank-biased social learning in a wild primate. *Sci. Rep.* 11, 9550. <https://doi.org/10.1038/s41598-021-88857-6>.
- B. Thierry, M. Singh, and W. Kaumanns, eds. (2004). *Macaque Societies: A Model for the Study of Social Organization*, 41 (Cambridge University Press).
- Boinski, S. (2005). *Macaque Societies: A Model of the Study of Social Organization*. Edited by Bernard Thierry, Mewa Singh and Werner Kaumanns. (Cambridge University Press). 2004. 418 pp. \$120.00 (cloth). ISBN 0-521-81847-8. *J. Mamm. Evol.* 12, 547–551. <https://doi.org/10.1007/s10914-005-7338-2>.
- Matsumura, S. (1999). The evolution of "egalitarian" and "despotic" social systems among macaques. *Primates* 40, 23–31. <https://doi.org/10.1007/BF02557699>.
- Cooper, E.B., Brent, L.J.N., Snyder-Mackler, N., Singh, M., SenGupta, A., Khatiwada, S., Malaivijitnond, S., Qi Hai, Z., and Higham, J.P. (2022). The rhesus macaque as a success story of the Anthropocene. *eLife* 11, e78169. <https://doi.org/10.7554/eLife.78169>.
- Bernstein, I.S. (1970). *Primate Status Hierarchies*. *Primate Behavior: Developments in Field and Laboratory Research* 1, pp. 71–109.
- Dubuc, C., Hughes, K.D., Cascio, J., and Santos, L.R. (2012). Social tolerance in a despotic primate: co-feeding between consortship partners in rhesus macaques. *Am. J. Phys. Anthropol.* 148, 73–80. <https://doi.org/10.1002/ajpa.22043>.
- Drews, C. (1993). The Concept and Definition of Dominance in Animal Behaviour. *Behaviour* 125, 283–313. <https://doi.org/10.1163/156853993X00290>.
- Dwartz, M.F., Curley, J.P., Tye, K.M., and Padilla-Coreano, N. (2022). Neural systems that facilitate the representation of social rank. *Philos. Trans. R. Soc. Lond. B Biol. Sci.* 377, 20200444. <https://doi.org/10.1098/rstb.2020.0444>.
- Higham, J.P., Pfefferle, D., Heistermann, M., Maestriperi, D., and Stevens, M. (2013). Signaling in multiple modalities in male rhesus macaques: sex skin coloration and barks in relation to androgen levels, social status, and mating behavior. *Behav. Ecol. Sociobiol.* 67, 1457–1469. <https://doi.org/10.1007/s00265-013-1521-x>.
- Gothard, K.M., Battaglia, F.P., Erickson, C.A., Spitzer, K.M., and Amaral, D.G. (2007). Neural responses to facial expression and face identity in the monkey amygdala. *J. Neurophysiol.* 97, 1671–1683. <https://doi.org/10.1152/jn.00714.2006>.
- Mosher, C.P., Zimmerman, P.E., and Gothard, K.M. (2011). Videos of conspecifics elicit interactive looking patterns and facial expressions in monkeys. *Behav. Neurosci.* 125, 639–652. <https://doi.org/10.1037/a0024264>.
- Minxha, J., Mosher, C., Morrow, J.K., Mamelak, A.N., Adolphs, R., Gothard, K.M., and Rutishauser, U. (2017). Fixations Gate Species-Specific Responses to Free Viewing of Faces in the Human and Macaque Amygdala. *Cell Rep.* 18, 878–891. <https://doi.org/10.1016/j.celrep.2016.12.083>.
- Brendel, W., Romo, R., and Machens, C.K. (2011). Demixed Principal Component Analysis. In *Advances in Neural Information Processing Systems*, 24, J. Shawe, R. Zemel, P. Bartlett, F. Pereira, and K.Q. Weinberger, eds., pp. 2654–2662.
- Kobak, D., Brendel, W., Constantinidis, C., Feierstein, C.E., Kepecs, A., Mainen, Z.F., Qi, X.L., Romo, R., Uchida, N., and Machens, C.K. (2016). Demixed principal component analysis of neural population data. *eLife* 5, e10989. <https://doi.org/10.7554/eLife.10989>.
- McNelis, N.L., and Boatright-Horowitz, S.L. (1998). Social monitoring in a primate group: the relationship between visual attention and hierarchical ranks. *Anim. Cogn.* 1, 65–69.
- Deaner, R.O., Khera, A.V., and Platt, M.L. (2005). Monkeys pay per view: adaptive valuation of social images by rhesus macaques. *Curr. Biol.* 15, 543–548. <https://doi.org/10.1016/j.cub.2005.01.044>.

34. Pannozzo, P.L., Phillips, K.A., Haas, M.E., and Mintz, E.M. (2007). Social Monitoring Reflects Dominance Relationships in a Small Captive Group of Brown Capuchin Monkeys (*Cebus apella*). *Ethology* *113*, 881–888. <https://doi.org/10.1111/j.1439-0310.2007.01392.x>.
35. Paukner, A., Slonecker, E.M., Murphy, A.M., Wooddell, L.J., and Dettmer, A.M. (2018). Sex and rank affect how infant rhesus macaques look at faces. *Dev. Psychobiol.* *60*, 187–193. <https://doi.org/10.1002/dev.21579>.
36. Foulsham, T., Cheng, J.T., Tracy, J.L., Henrich, J., and Kingstone, A. (2010). Gaze allocation in a dynamic situation: effects of social status and speaking. *Cognition* *117*, 319–331. <https://doi.org/10.1016/j.cognition.2010.09.003>.
37. Roberts, A., Palermo, R., and Visser, T.A.W. (2019). Effects of dominance and prestige based social status on competition for attentional resources. *Sci. Rep.* *9*, 2473. <https://doi.org/10.1038/s41598-019-39223-0>.
38. Maner, J.K., DeWall, C.N., and Gailliot, M.T. (2008). Selective attention to signs of success: Social dominance and early stage interpersonal perception. *Pers. Soc. Psychol. Bull.* *34*, 488–501. <https://doi.org/10.1177/0146167207311910>.
39. Setchell, J.M., and Dixon, A.F. (2001). Changes in the secondary sexual adornments of male mandrills (*Mandrillus sphinx*) are associated with gain and loss of alpha status. *Horm. Behav.* *39*, 177–184. <https://doi.org/10.1006/hbeh.2000.1628>.
40. Borgi, M., and Majolo, B. (2016). Facial width-to-height ratio relates to dominance style in the genus *Macaca*. *PeerJ* *4*, e1775. <https://doi.org/10.7717/peerj.1775>.
41. Altschul, D.M., Robinson, L.M., Coleman, K., Capitanio, J.P., and Wilson, V.A.D. (2019). An Exploration of the Relationships Among Facial Dimensions, Age, Sex, Dominance Status, and Personality in Rhesus Macaques (*Macaca mulatta*). *Int. J. Primatol.* *40*, 532–552. <https://doi.org/10.1007/s10764-019-00104-y>.
42. Rutishauser, U., Tudusciuc, O., Neumann, D., Mamelak, A.N., Heller, A.C., Ross, I.B., Philpott, L., Sutherling, W.W., and Adolphs, R. (2011). Single-unit responses selective for whole faces in the human amygdala. *Curr. Biol.* *21*, 1654–1660. <https://doi.org/10.1016/j.cub.2011.08.035>.
43. Rutishauser, U., Mamelak, A.N., and Adolphs, R. (2015). The primate amygdala in social perception - insights from electrophysiological recordings and stimulation. *Trends Neurosci.* *38*, 295–306. <https://doi.org/10.1016/j.tins.2015.03.001>.
44. Wang, F., Kessels, H.W., and Hu, H. (2014). The mouse that roared: neural mechanisms of social hierarchy. *Trends Neurosci.* *37*, 674–682. <https://doi.org/10.1016/j.tins.2014.07.005>.
45. Munuera, J., Rigotti, M., and Salzman, C.D. (2018). Shared neural coding for social hierarchy and reward value in primate amygdala. *Nat. Neurosci.* *21*, 415–423. <https://doi.org/10.1038/s41593-018-0082-8>.
46. Kumaran, D., Melo, H.L., and Duzel, E. (2012). The emergence and representation of knowledge about social and nonsocial hierarchies. *Neuron* *76*, 653–666. <https://doi.org/10.1016/j.neuron.2012.09.035>.
47. Rigotti, M., Ben Dayan Rubin, D.B.D., Wang, X.J., and Fusi, S. (2010). Internal Representation of Task Rules by Recurrent Dynamics: The Importance of the Diversity of Neural Responses. *Front. Comp. Neurosci.* *4*, 24. <https://doi.org/10.3389/fncom.2010.00024>.
48. Rigotti, M., Barak, O., Warden, M.R., Wang, X.J., Daw, N.D., Miller, E.K., and Fusi, S. (2013). The importance of mixed selectivity in complex cognitive tasks. *Nature* *497*, 585–590. <https://doi.org/10.1038/nature12160>.
49. Saez, A., Rigotti, M., Ostojic, S., Fusi, S., and Salzman, C.D. (2015). Abstract Context Representations in Primate Amygdala and Prefrontal Cortex. *Neuron* *87*, 869–881. <https://doi.org/10.1016/j.neuron.2015.07.024>.
50. O'Neill, P.K., Gore, F., and Salzman, C.D. (2018). Basolateral amygdala circuitry in positive and negative valence. *Curr. Opin. Neurobiol.* *49*, 175–183. <https://doi.org/10.1016/j.conb.2018.02.012>.
51. Gothard, K.M. (2020). Multidimensional processing in the amygdala. *Nat. Rev. Neurosci.* *21*, 565–575. <https://doi.org/10.1038/s41583-020-0350-y>.
52. Tye, K.M., Miller, E.K., Taschbach, F.H., Benna, M.K., Rigotti, M., and Fusi, S. (2024). Mixed selectivity: Cellular computations for complexity. *Neuron* *112*, 2289–2303. <https://doi.org/10.1016/j.neuron.2024.04.017>.
53. Mosher, C.P., Zimmerman, P.E., and Gothard, K.M. (2010). Response characteristics of basolateral and centromedial neurons in the primate amygdala. *J. Neurosci.* *30*, 16197–16207. <https://doi.org/10.1523/JNEUROSCI.3225-10.2010>.
54. Han, W., Tellez, L.A., Rangel, M.J., Jr., Motta, S.C., Zhang, X., Perez, I.O., Canteras, N.S., Shammah-Lagnado, S.J., van den Pol, A.N., and de Araujo, I.E. (2017). Integrated Control of Predatory Hunting by the Central Nucleus of the Amygdala. *Cell* *168*, 311–324.e18. <https://doi.org/10.1016/j.cell.2016.12.027>.
55. Martin, A.B., Cardenas, M.A., Andersen, R.K., Bowman, A.I., Hillier, E.A., Bensmaia, S., Fuglevand, A.J., and Gothard, K.M. (2023). A context-dependent switch from sensing to feeling in the primate amygdala. *Cell Rep.* *42*, 112056. <https://doi.org/10.1016/j.celrep.2023.112056>.
56. Rosvold, H.E., Mirsky, A.F., and Pribram, K.H. (1954). Influence of amygdectomy on social behavior in monkeys. *J. Comp. Physiol. Psychol.* *47*, 173–178. <https://doi.org/10.1037/h0058870>.
57. Kling, A., Lancaster, J., and Benitone, J. (1970). Amygdectomy in the free-ranging vervet (*Cercopithecus aethiops*). *J. Psychiatr. Res.* *7*, 191–199. [https://doi.org/10.1016/0022-3956\(70\)90006-3](https://doi.org/10.1016/0022-3956(70)90006-3).
58. Kling, A., and Cornell, R. (1971). Amygdectomy and social behavior in the caged stump-tailed macaque (*Macaca speciosa*). *Folia Primatol. (Basel)* *14*, 190–208. <https://doi.org/10.1159/000155350>.
59. Kalin, N.H., Shelton, S.E., Davidson, R.J., and Kelley, A.E. (2001). The primate amygdala mediates acute fear but not the behavioral and physiological components of anxious temperament. *J. Neurosci.* *21*, 2067–2074. <https://doi.org/10.1523/JNEUROSCI.21-06-02067.2001>.
60. Machado, C.J., and Bachevalier, J. (2006). The impact of selective amygdala, orbital frontal cortex, or hippocampal formation lesions on established social relationships in rhesus monkeys (*Macaca mulatta*). *Behav. Neurosci.* *120*, 761–786. <https://doi.org/10.1037/0735-7044.120.4.761>.
61. Bauman, M.D., Toscano, J.E., Mason, W.A., Lavenex, P., and Amaral, D.G. (2006). The expression of social dominance following neonatal lesions of the amygdala or hippocampus in rhesus monkeys (*Macaca mulatta*). *Behav. Neurosci.* *120*, 749–760. <https://doi.org/10.1037/0735-7044.120.4.749>.
62. Chang, S.W.C. (2013). Coordinate transformation approach to social interactions. *Front. Neurosci.* *7*, 147. <https://doi.org/10.3389/fnins.2013.00147>.
63. Sallet, J., Mars, R.B., Noonan, M.P., Andersson, J.L., O'Reilly, J.X., Jbabdi, S., Croxson, P.L., Jenkinson, M., Miller, K.L., and Rushworth, M.F. (2011). Social network size affects neural circuits in macaques. *Science* *334*, 697–700. <https://doi.org/10.1126/science.1210027>.
64. Noonan, M.P., Sallet, J., Mars, R.B., Neubert, F.X., O'Reilly, J.X., Andersson, J.L., Mitchell, A.S., Bell, A.H., Miller, K.L., and Rushworth, M.F.S. (2014). A neural circuit covarying with social hierarchy in macaques. *PLoS Biol.* *12*, e1001940. <https://doi.org/10.1371/journal.pbio.1001940>.
65. Utevsky, A.V., Smith, D.V., and Huettel, S.A. (2014). Precuneus is a functional core of the default-mode network. *J. Neurosci.* *34*, 932–940. <https://doi.org/10.1523/JNEUROSCI.4227-13.2014>.
66. Gianaros, P.J., and Manuck, S.B. (2010). Neurobiological pathways linking socioeconomic position and health. *Psychosom. Med.* *72*, 450–461. <https://doi.org/10.1097/PSY.0b013e3181e1a23c>.
67. Pachitariu, M., Steinmetz, N.A., Kadir, S.N., Carandini, M., and Harris, K.D. (2016). Fast and accurate spike sorting of high-channel count probes with KiloSort. In *Advances in Neural Information Processing Systems*, D. Lee, M. Sugiyama, U. Luxburg, I. Guyon, and R. Garnet, eds., pp. 4448–4456.

STAR★METHODS

KEY RESOURCES TABLE

| REAGENT or RESOURCE | SOURCE | IDENTIFIER |
|---|---|---|
| Critical commercial assays | | |
| Eye tracker | ISCAN Inc., ETL-200 | https://iscaninc.com/ |
| Headpost and grid | Gray Matter Research | https://www.graymatter-research.com/ |
| Microdrive system | Thomas Recording | https://www.thomasrecording.com/ |
| Electrodes | Plexon v-probes | https://plexon.com/products/plexon-v-probe/ |
| Neural data acquisition system | Plexon OmniPlex | https://plexon.com/plexon-systems/omniplex-neural-recording-system/ |
| Deposited data | | |
| Behavior data | This paper | https://doi.org/10.6084/m9.figshare.26952601 |
| Neural data | This paper | https://doi.org/10.6084/m9.figshare.26952631 |
| Experimental models: Organisms/strains | | |
| Macaca mulatta | California National Primate Research Center | N/A |
| Software and algorithms | | |
| Matlab | Mathworks | https://www.mathworks.com/ |
| Behavior and stimulus control tool | NIMH MonkeyLogic | https://monkeylogic.nimh.nih.gov/ |
| Data analysis codes | This paper | https://doi.org/10.6084/m9.figshare.26952712 |
| dPCA codes | Kobak et al. ³¹ | https://github.com/machenslab/dPCA |

EXPERIMENTAL MODEL AND STUDY PARTICIPANT DETAILS

Subject Details

We recorded single-unit spike activities in the amygdala, hippocampus, medial prefrontal cortex (mPFC), and other closely located areas from two adult male rhesus macaques (M_A : 10 years old, 13.6 kg; M_D : 9 years old, 11.8 kg). Meanwhile, we tracked the scan-path of these subjects as they watched visual stimuli (hierarchy and object movies). A shortcoming of the study was the limited size of our dataset due to an abdominal emergency (unrelated to the experimental procedures) developed by M_A . This animal was euthanized after only 5 recording sessions.

Video Stimuli

Each side of video clips had a resolution of 640 x 480 VGA, and these clips were combined to create the impression of 6 hierarchical interactions (AB, AC, AD, BC, BD, and CD) among a group of 4 monkeys. In this paper, we used four male hierarchy groups (P1, P3, P4 and P5. Where P stands for patriline). The juxtaposed movies were displayed on the screen at a resolution of 1920 x 1080 FHD and played for 6 or 15 seconds at a frame rate of 25 frames per second, resulting in each movie consisting of 125 or 375 frames. We manually segmented each monkey's facial and body area in all frames and manually scored the frames containing facial expressions. The number of pixels in the facial area compared to the body area is reported in [Table S1](#). Additionally, the number of frames with and without facial expressions is reported in [Table S2](#). Note that P4 and P5 were designed later than P1 and P3, with the intention of increasing the number of frames showing the animals with facial expressions. Therefore, we used only the looking time results from when the viewers watched the P1 and P3 hierarchies for analysis, as shown in [Figures 1D–1F](#). To control for social information, we prepared videos of moving objects that were formatted identically to the hierarchy movies. These videos featured the same four identical objects in each group and six different paired dyads, but without any actual interaction. Two macaque subjects participated in 20 recording sessions, with 15 of these sessions involving the object task blocks between or after hierarchy task blocks.

Task flow

Video timing (stimulus onset and offset) triggered by the subject's gaze on the starting cue was controlled using Monkey Logic (<https://monkeylogic.nimh.nih.gov/>). Each recording session (day) consists of several blocks, each containing 36 trials. Each trial began with a fixation of 250 ms on the 20 x 20 pixel-sized start cue, with a 100 x 100 pixel-sized invisible error boundary in the center

of the monitor. There was no restriction for where the monkeys looked, the subject could freely scan the video or look away. After the video played (either 15 s or 6 s in duration), the subject received a small drop of juice reward (the same amount for all videos). The subject monkeys were not subjected to food or fluid restriction.

METHOD DETAILS

Collecting Eye Tracking Data and Processing

Eye movements were recorded using an eye tracker (ETL-200, ISCAN Inc.) with a sampling rate of 120Hz. Eye tracker calibration was controlled by the hardware and software that provided by ISCAN Inc., and we calibrated the eye position at the beginning of each recording session. Eye tracking data was collected through voltage units, capturing both vertical and horizontal eye movements. To streamline analysis, we designated horizontal eye movement data as ‘Eye X’ and vertical data as ‘Eye Y’. As illustrated in [Figure S4A](#), raw data is initially recorded in millivolts (mV), then converted into pixel coordinates using calibration steps at the beginning of every recording session. Our method for pinpointing saccade or fixation onset leverages the energy of the signal (E), as detailed in [Equation 1](#), when X denotes the input signal, using $n=30$ as a window size. This proposed method highlights significant energy shifts, allowing us to distinguish between the saccadic and fixation periods. To determine the precise onset timing of saccades and fixations, we identify the onset by detecting when the second derivative of the energy signal crosses zero.

$$\left[E_t = \frac{\sum_{k=t-n}^{t+n} (X[k] - \mu_t)^2}{2n+1} \right]_{t=n+1}^{\text{length}(X)-n} \left(\text{when } \mu_t = \frac{\sum_{k=t-n}^{t+n} X[k]}{2n+1} \right) \quad (\text{Equation 1})$$

As mentioned, we used the eye tracking system with a sampling rate of 125Hz, indicating that the recording signal refreshes every 8 milliseconds on our data acquisition system (OmniPlex, Plexon Inc.), operates at a sampling rate of 1kHz. Since the eye tracking system has a lower resolution, there is a potential risk for timing inaccuracies of up to 8 milliseconds. To address this issue, we proposed the up-sampling approach outlined in [Equation 2](#). This method proves highly effective in mitigating existing challenges. In our analysis, when X denotes the input signal, we implemented $n=4$ as a window size.

$$X_{\text{upsampled}}[t] = \frac{\sum_{k=t-n}^{t+n} X[k]}{2n+1} \quad (\text{Equation 2})$$

As depicted results in [Figures S4B](#) and [S4C](#), the distributions of both saccade duration and fixation duration exhibit greater uniformity, with reductions in artifacts attributed to the lower sample rate (up to 8ms timing error) evident across all recording days. To juxtapose the original and up-sampled results, we employed the Kolmogorov-Smirnov test (KS test, utilized the Matlab function `kstest2`). Days where the p-value from the test falls below 0.05 are denoted with an asterisk (*). Given that saccade durations typically fall within the range of 20-60 ms, shorter than fixation durations spanning 60-600 ms, the impact of up-sampling is notably more pronounced in saccade duration distributions. This is reflected in the KS test results, demonstrating significantly different for all recording days in the saccade duration plots ([Figure S4B](#)).

Equations for the Looking Time Analysis

We measured the proportion of the looking time in [Figures 1D–1F](#). As below, we defined the equations for each panel to calculate the proper proportion of the looking time for each trial.

$$\text{In Figure 1D, } P_{\text{Dom}} = \frac{LT_{\text{Dom}}}{T_{\text{Movie}}}, P_{\text{Sub}} = \frac{LT_{\text{Sub}}}{T_{\text{Movie}}}$$

$$\text{In Figure 1E, } P_{\text{Dom\&FE}} = \frac{LT_{\text{Dom\&FE}}}{T_{\text{Dom\&FE}}}, P_{\text{Dom\&nFE}} = \frac{LT_{\text{Dom\&nFE}}}{T_{\text{Dom\&nFE}}}, P_{\text{Sub\&FE}} = \frac{LT_{\text{Sub\&FE}}}{T_{\text{Sub\&FE}}}, P_{\text{Sub\&nFE}} = \frac{LT_{\text{Sub\&nFE}}}{T_{\text{Sub\&nFE}}}$$

$$\text{In Figure 1F, } P_{\text{A\&NE}} = \frac{LT_{\text{A\&NE}}}{T_{\text{A\&NE}}}, P_{\text{B\&NE}} = \frac{LT_{\text{B\&NE}}}{T_{\text{B\&NE}}}, P_{\text{C\&NE}} = \frac{LT_{\text{C\&NE}}}{T_{\text{C\&NE}}}, P_{\text{D\&NE}} = \frac{LT_{\text{D\&NE}}}{T_{\text{D\&NE}}}$$

(When, P = Proportion of looking time, LT = Looking Time, T = Playing Time).

QUANTIFICATION AND STATISTICAL ANALYSIS

Single-unit Spike Recording and Identification of Stable Cells

Single-unit spiking activity was recorded using a linear electrode array (V-probe, Plexon Inc.) with 32 channels spaced at 200 μm intervals along a 260 μm diameter shaft. The target recording locations were determined based on pre-scanned magnetic resonance imaging (MRI) slices of each subject. We used a motorized micro-drive system (Thomas Motorized Electrode Manipulator (MEM), Thomas Recording), which has a 1 μm axial resolution, to advance the electrode.

We utilized KiloSort for spike sorting, following the methodology outlined by the literature.⁶⁷ For each sorted cell, we generated a cell specification sheet containing waveform data, inter-spike interval (ISI) histograms, spike count, ISI histogram stretched to the overall recording duration, and instantaneous firing rate throughout the recording session. Using a comprehensive list of criteria,

we assessed whether each spike train was suitable for further data analysis. For example, we assessed the stability of the instantaneous firing rate over the recording duration and filter out neurons with an average firing rate below 0.5Hz during task sessions. Also, neurons with fluctuating firing rates over a block of movie trials were eliminated. If a cell specification meets all criteria, we designate the neuron as a “good cell” and include it in further data analysis. In total, we collected “good cells” from 202 neurons in the amygdala (M_A : 106, M_D : 96).

Quantifying Cell Responses Tuned to Social Status and Partner Effect

We classified cells that exhibited a significant difference in firing rates ($FR = \frac{\text{Number of spikes}}{\text{Fixation duration}}$) when looking at dominant versus subordinate individuals as tuned to social status (see **Statistics** below). Similarly, if at least one of an attended target’s partners showed a significant difference in firing rates compared to the other two partners, we referred to this type of cell as tuned to the partner (partner effect). The PSTH plots in [Figures 2](#) and [4](#), we used a 10 ms bin for the spike counts for the histogram. We smoothed the signals in the PSTH plots solely for the purposes of better visualization, using Savitzky-Golay filtering (Matlab function *sgolayfilt*) with a polynomial order of 3 and a frame length of 11. Note that, we calculated statistics before applying the smoothing to the signals.

Statistics

In the PSTH plots, we used a t-test to assess the significant levels when comparing signals within the sliding window. The window size was 60 ms, and the stride size was 10 ms.

We used one-way and two-way ANOVA to statistically compare the effect of different on the firing rate of individual neurons. Significance levels (p-value) below 0.05, 0.01, and 0.001 are denoted with one, two, and three asterisks (*, **, ***), respectively.

We ran a one-way ANOVA to test for single factors. For example, we used it to compare looking times based on social status, the presence of facial expressions, facial area versus body area, and hierarchy rank. Additionally, we counted the number of neurons that were selective to the attended target’s social status or partner based on the results of the one-way ANOVA.

We utilized two-way ANOVA to explore how various factors affect neural activity in combination. To show the effects of the attended target’s identity and facial expressions, we conducted a two-way ANOVA with the factors of identity (monkey A, B, C, and D) and facial expressions (presence or absence of facial expressions). We also used a two-way ANOVA with the factors of social status (dominant and subordinate) and facial expressions (presence or absence of facial expressions) to test if the facial expressions of the fixated target affect neural activity instead of social status. Lastly, we tested for the main effect of status (dominant and subordinate), in addition to effect of identity (monkey B and C), using two-way ANOVA.

For both one-way and two-way ANOVA, we ran the analyses independently for each neuron to test the effect on neural activity.

We applied the dPCA model to recorded amygdala neurons to assess the impact of social status at the neuronal population level during both the social hierarchy task and the object control task. To compute dPCA results, we adapted Matlab package provided by literature³¹ (<https://github.com/machenslab/dPCA>) and customized its configurations for use with our datasets. We analyzed data from all 202 recorded amygdala neurons from two subjects during the hierarchy task ([Figures 3](#) and [S2](#)) and 162 of these neurons recorded during object task on the same days ([Figure S3](#)). To account for fixations of varying durations in the dPCA model, we normalized the spike timings from fixation onset to the duration of each fixation to a unit time of 1 second, segmented into 20 time points. We tested classification accuracy for 20 components, arranging them in descending order based on the explained variance for each marginalization. The classification accuracy value is derived from the 100 shuffling iterations. In the figures, we showed only the decoding accuracy plot corresponding to the highest-contributing component in the status factor results.

ADDITIONAL RESOURCES

There are no additional resources.

Visualizing Data Set Distributions

To visualize the distribution and probability density of each data set, we employed violin plots, which are hybrids of a box plots and kernel density plots. This method offers the advantage of depicting both summary statistics and the density of each variable. In our violin plots, the inner thick black box represents the interquartile range, while the inner thin black line expanding this box denotes 1.5 times the interquartile range. The white dot signifies the median point of the variables. The shaded area illustrates the probability density of the data variables, with thicker part indicating higher probability.